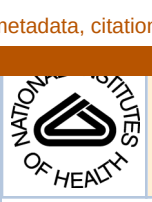

Published in final edited form as:

Environ Sci Technol. 2012 January 3; 46(1): 426–433. doi:10.1021/es202278s.

Mobilization of Manufactured Gas Plant Tar with Alkaline Flushing Solutions

Scott C. Hauswirth[*,†,‡], **Pamela Schultz Birak**[†], **Seth C. Rylander**[†], and **Cass T. Miller**[†]

Department of Environmental Sciences and Engineering, University of North Carolina at Chapel Hill, Chapel Hill, North Carolina

Abstract

This experimental study investigates the use of alkaline and alkaline-polymer solutions for the mobilization of former manufactured gas plant (FMGP) tars. Tar-aqueous interfacial tensions (IFTs) and contact angles were measured, and column flushing experiments were conducted. NaOH solutions (0.01–1 wt.%) were found to significantly reduce tar-aqueous IFT. Contact angles indicated a shift to strongly water-wet, then to tar-wet conditions as NaOH concentration increased. Column experiments were conducted with flushing solutions containing 0.2, 0.35, and 0.5% NaOH, both with and without xanthan gum (XG). Between 10 and 44% of the residual tar was removed by solutions containing only NaOH, while solutions containing both NaOH and XG removed 81–93% of the tar with final tar saturations as low as 0.018. The mechanism responsible for the tar removal is likely a combination of reduced IFT, a favorable viscosity ratio, and tar bank formation. Such an approach may have practical applications and would be significantly less expensive than surfactant-based methods.

Introduction

Former manufactured gas plants (FMGPs) were common in the U.S. and Europe between the early 1800s and the 1950s. These plants produced coke or town gas, a flammable gas that was used primarily for heating and lighting. The U.S. Environmental Protection Agency (EPA) estimated that there were between 36,121 and 55,001 FMGPs and related tar and gas processing facilities in the U.S. (1). The vast majority of these sites are suspected to have had releases of solid and liquid waste products, including tars, cyanide-bearing purifier waste, slag, and coke (1–3). The tars, which contain thousands of individual compounds, including many known or suspected carcinogens, are frequently the focus of remediation efforts at FMGPs (4). Polycyclic aromatic hydrocarbons (PAHs), hydrocarbons composed of two or more fused aromatic rings, are the dominant class of compounds in tars (5–8). Asphaltenes, operationally defined as the short-alkane insoluble fraction, are another important component of tars and may account for up to 36% of total tar mass (9, 10). Asphaltenes are suspected to play a key role in tar interfacial behavior (10–16).

Once released into a porous medium system, tars migrate downward by gravity, and because they are denser than water, can move down through the water table until reaching a

[*]To whom correspondence should be addressed shaus@email.unc.edu, Phone: (919) 966–6332. Fax: (919) 966–7911.
[†]University of North Carolina at Chapel Hill
[‡]CB# 7431, 148 Rosenau Hall, University of North Carolina at Chapel Hill, Chapel Hill, NC 27599

Supporting Information Available

Supporting information includes detailed descriptions of the methods used for the acid, base, and asphaltene extractions, diagrams of the experimental apparatus (Figures S1 and S2), a figure illustrating the change in pH during the IFT equilibration period (Figure S3), and plots of tar saturation versus PV flushed for the column experiments (Figures S4–S5). This material is available free of charge via the Internet at http://pubs.acs.org/.

confining layer (e.g., silt or clay). As the tar migrates through a porous medium, capillary forces act to trap isolated globules of tar in pores, creating a zone of residual saturation. FMGP tars' tendency toward NAPL-wetting conditions results in higher residual saturations than other denser-than-water NAPLs (DNAPLs), such as chlorinated solvents (3, 17). FMGP tars are persistent in the environment due to their resistance to chemical and biological degradation and the relatively low solubilities of many of the chemical constituents in these complex mixtures. The U.S. EPA estimated the per site clean-up costs in the millions of dollars, and a cumulative total of $128 billion for all of the FMGP and related sites in the U.S. (1). A number of strategies have been applied or investigated for MGP tar remediation including containment, excavation, natural or enhanced bioremediation, extraction by pumping (with or without the use of chemical additives), chemical oxidation, and thermal methods (1, 3, 18–27).

Mobilization approaches are attractive alternatives for the remediation of NAPLs since they are less restricted by site access limitations than other methods. The basic principle behind such methods is to reduce the forces trapping the NAPL in the porous media. NAPL droplets are trapped in porous media when capillary forces are greater than the pressure acting on the drop. The capillary number (N_C) is a dimensionless number that represents the ratio of viscous forces to capillary forces, and for vertical flow it is defined as follows (28):

$$N_C = \frac{q_\alpha \mu_\alpha}{\sigma_{\alpha n} \cos\theta}, \quad (1)$$

where q_a is the magnitude of the aqueous phase Darcy velocity, μ_a is the aqueous phase viscosity, θ is the contact angle, and σ_{an} is the interfacial tension (IFT) between the aqueous and NAPL phases. When buoyancy forces are expected to be important, N_C may also be combined with the bond number (N_B) to arrive at the trapping number (N_T), which, for vertical flow, is defined as follows (28):

$$N_T = \left| N_C + \frac{g k k_{r\alpha} \Delta\rho}{\sigma_{\alpha n} \cos\theta} \right| = |N_C + N_B|, \quad (2)$$

where k is the intrinsic permeability, k_{ra} is the relative water permeability, g is gravitational acceleration, and $\Delta\rho = \rho_a - \rho_n$, where ρ_a and ρ_n are the aqueous and NAPL phase densities. When $\Delta\rho$ is small, as is the case for many FMGP tar-water systems, the contribution of N_B is negligible relative to N_C. It has been well established that residual saturation is a decreasing function of the trapping number (28, 29). The goal for a mobilization-based remediation technique is to increase N_T, which is typically accomplished by reducing σ_{an} by adding cosolvents or surfactants to the aqueous flushing solution, or by increasing the flow rate. The addition of polymers, such as xanthan gum (XG), to increase μ_a is common in the petroleum industry for enhanced oil recovery (EOR) applications (30), but has seen less use in the remediation field. Investigations of the effect of viscosity on remediation efficiency have tended to focus on the viscosity ratio ($\kappa = \mu_n/\mu_a$) alone, rather than in relation to capillary forces. Giese and Powers (31) performed creosote and synthetic NAPL flushing experiments with XG solutions under NAPL-wet conditions, and found that solutions with $\kappa = 0.1$ resulted in final NAPL saturations roughly half those obtained when using solutions with $\kappa \geq 1$. Tzimas et al. (32) reported a similarly strong impact for other NAPLs. Some researchers have found that $N_C \kappa^m$, where m is determined by fitting to experimental data, correlates with residual NAPL saturations better than N_C alone (33). The proposed reason for this is that μ_n, which is not accounted for in the formulation of N_C, impacts NAPL entrapment processes (i.e., snap-off).

The use of alkaline agents to reduce IFT was developed by petroleum researchers for EOR applications. When exposed to high pH aqueous solutions, organic acids in crude oils become ionized, forming natural surfactants that significantly reduce the NAPL-water IFT (34–37). One of the major advantages of this approach is cost: commonly used alkaline chemicals, sodium hydroxide (NaOH) and sodium carbonate (Na_2CO_3), are readily available and inexpensive compared to other flushing chemicals such as surfactants (38, 39). From a remediation perspective, an additional benefit is that both NaOH and Na_2CO_3 are designated as “generally recognized as safe” by the U.S. FDA and used widely as food additives (40). The feasibility of applying such alkaline-based approaches to the remediation of FMGP tars has not been explicitly investigated; however, it has been shown that when exposed to high pH solutions, FMGP tars exhibit lower NAPL-water IFT and have a decreased tendency to wet porous media (10–16). This evidence suggests that acidic species are present that react to form surface active compounds, and that alkaline flushing may be effective for tars.

Two field trials of alkaline-surfactant-polymer (ASP) flushing have been conducted on wood-treating creosote, a DNAPL with similarities to, but important differences from, FMGP tars. One of the trials failed due to injection problems and insufficient site characterization, while the other trial successfully removed 84.3% of the residual creosote (41–43). The latter study, however, used a five-stage sequence of chemical flushing solutions and relied more on the use of surfactants than alkaline agents. The surfactant concentration in the main flushing solution was 1.4% while the pH was only 9.2; alkaline flushing solutions for EOR applications are typically above pH 12 (30).

The objectives of this work are: (1) to assess the impact of NaOH solutions on the IFT and contact angle of FMGP tars, (2) to conduct column experiments to assess the potential for the use of such solutions to remediate FMGP tars, and (3) to assess the impact of the remediation on dissolved phase concentrations of 15 PAHs.

Materials and Methods

All solvents used were ACS Reagent grade or better (Fisher) and water was distilled and deionized (DDI). Stock solutions of 10% NaOH (99.8%; Fisher Scientific) and 5% XG (MP Biomedicals) were prepared and used to make all subsequent solutions for IFT, contact angle, and flushing experiments. The buffer solution was made by dissolving appropriate quantities of NaH_2PO_4 and Na_2HPO_4 in DDI and titrating to pH 7 to produce a 100 mM stock solution. This solution was diluted to 1 mM, and NaCl was added to adjust the ionic strength to 10 mM. The tar used for this study was a tar, believed to be a carburetted water-gas tar, collected from a well at an FMGP in Baltimore, Maryland, USA. Measurements of pH were made with an Orion Research EA 940 expandable ion meter. All experiments were conducted at 22 ± 1 °C.

Fluid Characterization

To determine the tar composition, 0.05 g of tar was dissolved in 10 mL dichloromethane (DCM) containing 2-fluorobiphenyl and m-terphenyl as internal standards. Twenty-six compounds, including the 16 EPA priority pollutant PAHs, were quantified using a Hewlett-Packard 5890 gas chromatograph equipped with a flame ionization detector (GC-FID) and a Hewlett-Packard 7673 autoinjector system. Peak identification was confirmed with a gas chromatograph equipped with a mass spectrum detector (GC-MS). The GC-FID was calibrated with six standard solutions containing concentrations ranging from 0.3 to 500 mg/L.

Asphaltenes were extracted with n-pentane and reprecipitated from toluene. Acids and bases were extracted with 1 M NaOH and 10% H_2SO_4, respectively. Details of the methods used for the asphaltene, acid, and base extractions are provided in Supporting Information.

Density was measured with an Anton Paar DMA 48 density meter. Tar dynamic viscosity (μ_t) was measured with a TA Instruments AR-G2 rheometer at a shear rate of 1 s^{-1}. The viscosity of XG solutions with 0, 0.2, and 0.5% NaOH was measured over a shear rate ($\dot{\gamma}$) range of 10^{-4} to 10 s^{-1}. The solutions containing NaOH were analyzed within 1 hour of being produced.

IFT and Contact Angle

IFT was measured using the pendant drop method. An optical glass cell (Krüss) was filled with aqueous solution (0–1 wt.% NaOH), and a drop of tar was suspended from a stainless steel needle. A digital video camera captured images of the drop, and Krüss's Drop Shape Analysis II (DSA2) software was used to determine the native IFT, for which $\Delta\rho$ =1 g/cm^3. The density of each phase was measured and used to determine the actual IFT. A schematic of the experimental apparatus is provided in Supporting Information.

Two needle sizes were used, a 16-gauge needle (1.6-mm outer diameter) for IFTs above 1 mN/m, and a 24-gauge needle (0.4-mm diameter) for IFTs between 1 mN/m and 0.05 mN/m, which was the lower limit of quantification for this method. The magnification of the optics system was adjusted as appropriate for each needle size. Optical scale calibration was performed directly by the DSA2 software using needle diameters measured to 0.001 mm with a digital micrometer. DCM-distilled water interfacial tensions were measured as a check of the accuracy of the measurements.

IFT was measured with and without prior equilibration. Equilibration entailed combining the tar and aqueous solution at a 1:3 volume ratio in a centrifuge tube, shaking periodically over a period of 7 days, and centrifuging at 3200 rpm (1700 g) for 20 minutes prior to measurement. This volume ratio was chosen based on an assumed residual tar saturation of 0.25 for the column experiments.

Contact angles were measured using the same instrumentation and software as for the IFT measurements. The measurements were conducted on a 25 mm × 25 mm quartz slide (Chemglass) placed in the glass cell. The interaction between the tar and the needle used to dispense the drop was found to greatly impact the drop shape, and therefore an inclined plate method was used to determine the advancing (θ_A) and receding (θ_R) contact angles. A drop was dispensed on the quartz slide and the stage was tilted until the drop just began to move along the surface of the slide. Images captured immediately prior to the movement of the drop were used to measure the angle (through the aqueous phase) on each side of the drop. Contact angle measurements were conducted with the equilibrated tar and aqueous phases.

Between each sample, the glass cell and quartz slide were rinsed sequentially with methanol, n-methylpyrollidinone (NMP), DCM, methanol, and DDI water, followed by a 15 min soak in NaOH-saturated ethanol and a final, thorough DDI rinse.

Column Studies

Column studies were conducted in 2.5-cm inner diameter glass columns that were adjusted to 10 cm in length. The influent and effluent tubing, along with all associated fittings, were constructed of PTFE. Water and flushing solutions were pumped using Harvard Apparatus PHD 4400 programmable syringe pumps. A schematic of the column apparatus is provided in Supporting Information.

The columns were dry packed with a sieved fraction (#25 to #35 mesh) of a natural quartz and feldspar sand, using an air vibrator to ensure complete compaction. This sand was used since it is more representative of natural mineralogy and grain shapes than glass beads or pure quartz sand that are commonly used for this type of experiment. The intrinsic permeability was determined to be $2.2\pm0.4 \times 10^{-7}$ cm^2 for a representative column by measuring the head difference between the inlet and outlet over a range of flow rates. Further characterization of the original soil is presented elsewhere (44). After packing, the column was flushed upward with carbon dioxide for 30 minutes at a rate of 20–30 mL/min to displace the air from the column. This was followed by a several pore volume flush of pH 7 buffer to displace and dissolve the carbon dioxide. Porosity was calculated for each column based on the bulk density.

Tar was injected upward into the column to achieve a NAPL saturation (S_n) approaching 1. A water flood was conducted to create a residual tar saturation by flushing the pH 7 buffer downward until tar was no longer present in the effluent. Column experiments were conducted using 0.2, 0.35, and 0.5% NaOH solutions with and without the addition of 5000 ppm XG. An additional column was flushed with a 5000 ppm XG solution without NaOH. Chemical flushes were conducted in a downward direction and performed until no tar was present in the effluent. The column was then flushed with several pore volumes of the pH 7 buffer. Effluent samples of between 5 and 30 mL were collected during the water and chemical flushing. Tar removal was quantified by extracting the tar in the effluent samples with sequential portions of DCM, centrifuging and pipetting off the organic phase between each step, and analyzing the extract by GC-FID as described above. Internal standards were added directly to the effluent samples to account for extraction losses and matrix background. The mass of six individual compounds (naphthalene, 1- and 2-methylnaphthalene, acenaphthene, fluorene, phenanthrene) in each sample was determined and divided by the known mass fraction of that compound in the tar. These six values were averaged to provide an estimate of the tar mass in the sample. This approach was tested by adding a known mass of tar to DDI-filled centrifuge vials, and extracting as for the samples. These tests indicated that such an approach was accurate to within 0.4%.

Aqueous-phase concentrations of PAHs were measured before and after the alkaline flushing for select columns. Aqueous effluent samples were collected in acetonitrile containing deuterated anthracene as an internal standard. The samples were filtered with 0.2 μm PTFE syringe filters (Fisher), allowing the first 1 mL to go to waste. Analysis was performed by high-performance liquid chromatography (HPLC) (Waters 600S controller, 616 pump, and 717 autosampler) equipped with a multi-wavelength fluorescence detector (Waters 2475) as described in (45).

At the completion of the flushing, the soil was split into four segments along the length of the column, each of which was homogenized and divided into three centrifuge vials. Internal standard and Na_2SO_4 (10 g) were added, and the tar was extracted with one 15-mL and three 10-mL portions of DCM. The vials were shaken and centrifuged between each step, and the supernatant from each sample was combined and diluted to 50 mL. The samples were then analyzed by GC-FID.

Results

The tar composition is presented in Table 1. The density of the tar was 1.0800 ± 0.0004 g/cm^3 (22°C), and the dynamic viscosity was 190 ± 10 (22°C, 1 s^{-1}). Rheological measurements of 5000 ppm XG solutions with 0.5% NaOH and without NaOH are shown in Figure 1. The solution containing 0.2% NaOH yielded results very similar to those of the 0.5% solution. The addition of NaOH resulted in a significant reduction of the viscosity. At

0.75 s^{-1}, the shear rate ($\dot{\gamma}$) estimated to occur in the column using the equation of Hirasaki and Pope (46), the viscosity is a factor of 2.7 lower for the solution containing NaOH than the pure XG solution.

IFT and Contact Angle

The measured IFT for DCM in DDI was 27.7 ± 0.6 mN/m (n=7), in good agreement with literature values, which ranged from 27.4–28.3 mN/m (47–51). The IFT from (47) was measured at 20°C, while all other literature values were reportedly measured at room temperature.

The dynamic IFT for unequilibrated tar samples was measured for NaOH ranging from 0.1–1%. A 0.01% NaOH solution was also tested, but the initial IFT was below the quantitative limit of the method. The unequilibrated samples showed significant changes in IFT with time (Figure 2). Initially, the results show a trend of increasing IFT with increasing NaOH concentration. The trend begins to change at t ≈ 2 min; however, difficulties with drops releasing from the needle prevented measurement of IFT for some NaOH concentrations over longer time scales.

Equilibrium IFT was found to decrease steadily as the NaOH concentration was increased from 0 to 0.5% (Figure 3). The IFT changed little between 0.5 and 1%. IFTs for equilibrated samples with NaOH concentrations of 0.1–0.4% were significantly higher than the corresponding non-equilibrated samples. The pH of the solutions was not significantly altered during the equilibration period, except for the 0.01% solution which exhibited a pH reduction from 11.40 to 9.88 (see figure in Supporting Information).

The results of the contact angle analyses are shown in Figure 4. With the pH 7 buffer, contact angles were θ_R = 71 ± 2°and θ_A = 18 ± 7°. NaOH solutions of 0.01–0.3% resulted in much lower θ_R values, approximately 20°, while the θ_A values were similar to that of the buffer. At 0.4% NaOH, θ_A remained low, but θ_R increased significantly to about 70°. The maximum receding angle (137±9°) occurred at an NaOH concentration of 0.5%, with similarly high values measured for 0.7 and 1% NaOH solutions. Advancing angles for 0.5–1% NaOH solutions ranged from 35–70°. The results indicate that the lower NaOH concentrations (0.01–0.3%) reduce the NAPL-wetting tendency of the system, while the higher concentrations (0.4–1%) increase it. Drummond and Israelachvili (52) reported a similar shift toward NAPL-wetting for crude oils at high pH and sodium concentrations. The reported cause of the shift is a combination of the reduction of IFT associated with the high pH and the reduction of repulsive forces between the NAPL and solid phase resulting from the high Na^+ concentration.

Column Studies

The results of the column experiments are summarized in Table 2 and plots of residual saturation versus pore volumes (PV) flushed for select columns are provided in Figure 5 (see Supporting Information for plots of additional columns). The column experiments conducted without XG (C1–C3) resulted in relatively low removal efficiencies. The 0.2 (C1) and 0.5% (C3) NaOH solutions removed only 15 and 10% of the residual tar, respectively. The majority of the tar removed by these columns eluted during the first 2 PV of the alkaline flushing. The formation of a NAPL bank was observed in both of these columns immediately after the injection of alkaline solution, but appeared to stall near the top of the column. Column C2 (0.35% NaOH) resulted in a considerably higher tar removal (44%), but required approximately 7 PV to do so. The NAPL bank in this column was visibly more robust than those in C1 and C3, but also became unstable near the top of the column and failed to uniformly pass through the column.

Column C4 was conducted with 5000 ppm XG without NaOH to determine the impact of an increased flushing solution viscosity. This column resulted in the removal of 51% of the residual tar and a final tar saturation of 0.13.

Columns C5–C10 were all flushed with solutions containing an XG concentration of 5000 ppm and varying NaOH concentrations of 0.2% (C5–C6), 0.35% (C7), and 0.5% (C8–C10). The viscosity ratio for these columns was about 0.1 at $\dot{\gamma} = 0.75$. The lowest final tar saturation (0.018, 93% removal) was obtained for a column flushed with a 0.2% NaOH solution (C5). A duplicate of this column (C6) resulted in a higher 0.037 tar saturation, apparently due to a small amount of tar trapped along the wall of the column. The columns flushed with 0.5% NaOH had somewhat higher final saturations, ranging from 0.043–0.048. Stable NAPL banks were observed in columns C5–C10, and were responsible for the large majority of the tar removal.

Aqueous phase concentrations of 15 PAHs were measured before and after alkaline flushing for columns C8–C10. Table 3 shows the results from column C9, which are typical of the results from the other columns. With the exception of naphthalene, statistically significant reductions in aqueous phase concentrations were not observed.

Discussion

Consistent with previous MGP tar studies, tar-aqueous IFTs were found to be significantly lower at higher pH than at neutral pH (10, 11). This work, however, differs from previous studies in that a higher range of pH (7–13.4) was investigated. Instantaneous measurements indicated that, after a large decrease between pH 7 and 11.40, IFT generally increased with increasing NaOH concentration over this range. Measurements of equilibrated samples, however, showed that lower concentrations of NaOH resulted in relatively high IFTs. At an NaOH concentration of 0.1%, for example, there is a difference of two orders of magnitude between the instantaneous and equilibrium IFT. The difference between instantaneous and equilibrium IFT is much less for solutions with higher NaOH concentrations (0.5–1%). The change in pH during the equilibration period was minimal for all but the 0.01% NaOH solution, indicating that other mechanisms are responsible for the observed behavior.

A number of petroleum researchers have investigated the dynamic IFT behavior of crude oils or synthetic oil-acid mixtures contacted with alkaline solutions (35, 39, 55–59). The basic mechanisms described in these studies are as follows. The organic acids (HA) present in the oil or tar are deprotonated at the interface, resulting in a reduction of IFT. The ionized acids (A^-) may subsequently diffuse into the bulk aqueous phase or combine with Na^+ ions to form surface-inactive soap molecules (NaA). The rates and equilibria associated with these processes are responsible for dynamic IFT behavior. The differences between instantaneous and equilibrium IFT at different NaOH concentrations observed in this study could be explained by the higher ionic strength of the 0.5–1% NaOH solutions suppressing the diffusion of A^- away from the interface. However, the formation of NaA would simultaneously be expected to increase, leading to an increase in IFT. An alternate explanation relates to the presence of multiple acidic species within the tar. Chiwetelu et al. (55) showed that the dominant interfacially active species changed from a higher solubility, lower pK_a acid to a less soluble, higher pK_a acid as NaOH concentration was increased. A more recent study (37) found that higher molecular weight petroleum acid fractions required a higher alkaline concentration to produce an IFT reduction, but resulted in much less time-dependent IFTs as compared to the lower molecular weight fractions. It is likely that a similar range of species is present in FMGP tars and contributes to the observed differences in dynamic IFT behavior at different NaOH concentrations.

The columns conducted without XG indicate that the reduction of IFT does result in the mobilization of tar, but that the amount of removal is not correlated with either the instantaneous or equilibrium IFT values. The column flushed with 0.35% NaOH, which had intermediate equilibrium and instantaneous IFTs, resulted in a significantly lower final saturation than both the 0.2% NaOH column (with a lower instantaneous IFT) and the 0.5% NaOH column (with a lower equilibrium IFT). NAPL-wet conditions are associated with reduced NAPL recovery, potentially explaining the low recovery for the 0.5% NaOH solution, which exhibited a high contact angle (16, 60). The reason for the limited effectiveness of the 0.2% NaOH flushing solution is not immediately clear. A study investigating alkaline flushing for a heavy crude oil similarly reported that the solution producing the minimum IFT was ineffective and that a higher alkaline concentration was required (61). Interactions between the alkaline solution and the solid phase (i.e., silica dissolution, ion exchange), and the increase of IFT as equilibration occurs likely play a role.

The addition of XG to the flushing solutions greatly improved tar removal, with final tar saturations below 0.05 for all NaOH concentrations. The final tar saturations for 0.2 and 0.35% NaOH were similar, ranging from 0.018 to 0.037. The slightly higher final saturation in the 0.5% NaOH columns may be due to the high contact angles observed at this NaOH concentration. The addition of XG not only increases the viscous forces acting on NAPL droplets, directly resulting in increased tar mobilization, but also greatly reduces instabilities in the flushing front, decreasing flow bypassing, and improving NAPL bank formation. Based on the results of the column experiments, it is clear that the combination of IFT reduction and increased flushing fluid viscosity results in much more effective tar removal than either mechanism alone.

The use of NaOH-XG flushing solutions successfully removed between 81–93% of the residual tar within about 1.5 PV without the use of costly surfactants. Although several obstacles exist, such a method may have a place in the remediation of MGP sites. As is the case with all mobilization-based methods, complete removal of contaminants is not attained, with final saturations of 0.018–0.048. At these saturations, aqueous phase PAH concentrations would not be expected to be significantly reduced (62), and secondary remediation techniques, such as cosolvent flushing, *in situ* chemical oxidation (ISCO), or bioremediation would likely be required to achieve remediation goals.

Supplementary Material

Refer to Web version on PubMed Central for supplementary material.

Acknowledgments

The authors wish to thank Dr. Joseph Pedit for his assistance in preparing the column apparatus and with general laboratory procedures. This work was supported by National Institute of Environmental Health Sciences grant 5 P42 ES05948.

References

1. U.S. EPA. Cleaning Up the Nation’s Waste Sites: Markets and Technology Trends. 2004. EPA/542/R-04/015
2. Harkins, SM.; Truesdale, RS.; Hill, R.; Hoffman, P.; Winters, S. US production of manufactured gases: Assessment of past disposal practices. Prepared by Research Triangle Institute for the U.S. Environmental Protection Agency, Hazardous Waste Engineering Research Laboratory; Cincinnati, OH. 1988.

3. Luthy RG, Dzombak DA, Peters CA, Roy SB, Ramaswami A, Nakles DV, Nott BR. Remediating tar-contaminated soils at manufactured gas plant sites. Environmental Science & Technology. 1994; 28:266A–276A.
4. NIOSH. Criteria for a recommended standard: Occupational exposure to coal tar products. U.S. Dept. of Health, Education, and Welfare, Public Health Service; Center for Disease Control; National Institute for Occupational Safety and Health; Cincinnati: 1977.
5. Zhang MJ, Chen BJ, Shen SD, Chen SY. Compositional studies of high-temperature coal tar by GC–FT–IR analysis of middle oil fractions. Fuel. 1997; 76:415–423.
6. Zhang MJ, Li SD, Chen BJ. Compositional studies of high-temperature coal-tar by GC/FTIR analysis of light oil fractions. Chromatographia. 1992; 33:138–146.
7. Wise S, Sander L, Chang H, Markides K, Lee M. Shape selectivity in liquid and gas chromatography: Polymeric octadecylsilane (C18) and liquid crystalline stationary phases. Chromatographia. 1988; 25:473–479.
8. Blanco CG, Blanco J, Bernad P, Guillen MD. Capillary gas chromatographic and combined gas chromatography–mass spectrometric study of the volatile fraction of a coal tar pitch using OV-1701 stationary phase. Journal of Chromatography A. 1991; 539:157–167.
9. Birak PS, Miller CT. Dense non-aqueous phase liquids at former manufactured gas plants: Challenges to modeling and remediation. Journal of Contaminant Hydrology. 2009; 105:81–172. [PubMed: 19176266]
10. Zheng JZ, Powers SE. Identifying the effect of polar constituents in coal-derived NAPLs on interfacial tension. Environmental Science & Technology. 2003; 37:3090–3094. [PubMed: 12901655]
11. Barranco FT, Dawson HE. Influence of aqueous pH on the interfacial properties of coal tar. Environmental Science & Technology. 1999; 33:1598–1603.
12. Powers SE, Anckner WH, Seacord TF. Wettability of NAPL-contaminated sands. Journal of Environmental Engineering - ASCE. 1996; 122:889–896.
13. Zheng JZ, Powers SE. Organic bases in NAPLs and their impact on wettability. Journal of Contaminant Hydrology. 1999; 39:161–181.
14. Zheng JZ, Shao JH, Powers SE. Asphaltenes from coal tar and creosote: Their role in reversing the wettability of aquifer systems. Journal of Colloid and Interface Science. 2001; 244:365–371.
15. Zheng JZ, Behrens SH, Borkovec M, Powers SE. Predicting the wettability of quartz surfaces exposed to dense nonaqueous phase liquids. Environmental Science & Technology. 2001; 35:2207–2213. [PubMed: 11414020]
16. Hugaboom DA, Powers SE. Recovery of coal tar and creosote from porous media: The influence of wettability. Ground Water Monitoring and Remediation. 2002; 22:83–90.
17. Villaume JF. Investigations at sites contaminated with dense non-aqueous phase liquids. Ground Water Monitoring Review. 1985; 5:60–74.
18. Wu J, Gong Z, Zheng L, Yi Y, Jin J, Li X, Li P. Removal of high concentrations of polycyclic aromatic hydrocarbons from contaminated soil by biodiesel. Frontiers of Environmental Science & Engineering in China. 2010; 4:387–394.
19. Troxler WL, Brankley TW. Factors affecting soil clean-up levels achievable by thermal desorption technologies at MGP sites. Land Contamination & Reclamation. 2006; 14:209–217.
20. Mival K, Pump W, Dixon G. From wasteland to green parkland, the remediation of the former West Melbourne Gasworks, Victoria, Australia. Land Contamination & Reclamation. 2006; 14:194–199.
21. Lingle JW, Brehm KL. Application of source removal and natural attenuation remediation strategies at MGP sites in Wisconsin. Remediation Journal. 2003; 13:29–39.
22. Heasman I, Westcott FJ. Remediation of a gasworks site for residential development: The Wharf Lane Site, Solihull, UK. Land Contamination & Reclamation. 2006; 14:189–193.
23. Grosscurth M, Osten M, Kilger R. Clean-up of the Grasbrook Gasworks in the HafenCity of Hamburg. Land Contamination & Reclamation. 2006; 14:185–188.
24. U.S. EPA. Waste Research Strategy. 1999.

25. Switzer C, Pironi P, Gerhard JI, Rein G, Torero JL. Self-sustaining smoldering combustion: A novel remediation process for non-aqueous-phase liquids in porous media. Environmental Science & Technology. 2009; 43:5871–5877. [PubMed: 19731690]
26. Baker RS, Brogan D, Lotti M. Demonstration of tailored levels of in-situ heating for remediation of a former MGP site. Land Contamination and Reclamation. 2006; 14:335–339.
27. Johnson, J.; LA; Fahy, LJ. In situ treatment of manufactured gas plant contaminated soils demonstration program. 1997.
28. Pennell KD, Pope GA, Abriola LM. Influence of viscous and buoyancy forces on the mobilization of residual tetrachloroethylene during surfactant flushing. Environmental Science & Technology. 1996; 30:1328–1335.
29. Pope, GA.; Wade, WH. In Surfactant-Enhanced Subsurface Remediation: Emerging Technologies. Sabatini, DA.; Knox, RC.; Harwell, J., editors. American Chemical Society; Washington, D.C: 1995. p. 142-160.
30. Sheng, JJ. Modern Chemical Enhanced Oil Recovery. Gulf Professional Publishing (Elsevier); Burlington, MA: 2011.
31. Giese SW, Powers SE. Using polymer solutions to enhance recovery of mobile coal tar and creosote DNAPLs. Journal of Contaminant Hydrology. 2002; 58:147–167. [PubMed: 12236554]
32. Tzimas G, Matsuura T, Avraam D, Van der Brugghen W, Constantinides GN, Payatakes A. The combined effect of the viscosity ratio and the wettability during forced imbibition through nonplanar porous media. Journal of Colloid and Interface Science. 1997; 189:27–36.
33. Longino BL, Kueper BH. Effects of capillary pressure and use of polymer solutions on dense, non-aqueous-phase liquid retention and mobilization in a rough-walled fracture. Environmental Science and Technology. 1999; 33:2447–2455.
34. Chiwetelu CI, Hornof V, Neale GH, George A. Use of mixed surfactants to improve the transient interfacial tension behaviour of heavy oil/alkaline systems. The Canadian Journal of Chemical Engineering. 1994; 72:534–540.
35. Chiwetelu CI, Hornof V, Neale GH. Mechanisms for the interfacial reaction between acidic oils and alkaline reagents. Chemical Engineering Science. 1990; 45:627–638.
36. Islam MR, Chakma A. Mathematical modelling of enchanced oil recovery by alkali solutions in the presence of cosurfactant and polymer. Journal of Petroleum Science and Engineering. 1991; 5:105–126.
37. Zhang L, Luo L, Zhao S, Xu ZC, An JY, Yu JY. Effect of different acidic fractions in crude oil on dynamic interfacial tensions in surfactant/alkali/model oil systems. Journal of Petroleum Science and Engineering. 2004; 41:189–198.
38. Taylor, KC.; Hawkins, BF. In Emulsions: Fundamentals and Applications in the Petroleum Industry. Schramm, LL., editor. American Chemical Society; Washington, D.C: 1992. p. 263-294.
39. Elkamel A, Al-Sahhaf T, Suttar Ahmed A. Studying the interaction between an Arabian heavy crude oil and alkaline solutions. Petroleum Science and Technology. 2002; 20:789–807.
40. U.S. Department of Health and Human Services. CFR Title 21, Part 184 Direct Food Substances Generally Recognized as Safe. 2002.
41. Roote, DS. Prepared by Ground-Water Remediation Technologies Analysis Center. 1998. Technology Status Report: In Situ Flushing. TS-98-01
42. Mulligan CN, Yong RN, Gibbs BF. Surfactant-enhanced remediation of contaminated soil: A review. Engineering Geology. 2001; 60:371–380.
43. Pitts, M.; Wyatt, K.; Sale, T.; Piontek, KR. SPE International Symposium on Oilfield Chemistry; Society of Petroleum Engineers; New Orleans, LA, USA. 1993. p. 33-44.
44. Ball WP, Liu C, Xia G, Young DF. A diffusion-based interpretation of tetrachloroethene and trichloroethene concentration profiles in a groundwater aquitard. Water Resources Research. 1997; 33:2741–2757.
45. Birak PS, Newman AP, Richardson SD, Hauswirth SC, Pedit JA, Aitken MD, Miller CT. Cosolvent flushing for the remediation of PAHs from former manufactured gas plants. Journal of Contaminant Hydrology. 2011 In Press.

46. Hirasaki GJ, Pope GA. Analysis of factors influencing mobility and adsorption in the flow of polymer solution through porous media. Society of Petroleum Engineers Journal. 1974; 14:337–346.
47. Freitas AA, Quina FH, Carroll FA. Estimation of water-organic interfacial tensions. A linear free energy relationship analysis of interfacial adhesion. Journal of Physical Chemistry B. 1997; 101:7488–7493.
48. Bahramian A, Danesh A. Prediction of liquid–liquid interfacial tension in multi-component systems. Journal of Fluid Phase Equilibria. 2004; 221:197–205.
49. Sah H, Choi S-K, Choi H-G, Yong C-S. Relation of dynamic changes in interfacial tension to protein destabilization upon emulsification. Archives of Pharmacal Research. 2002; 25:381–386.10.1007/BF02976643 [PubMed: 12135114]
50. Sah H. Protein behavior at the water/methylene chloride interface. Journal of Pharmaceutical Sciences. 1999; 88:1320–1325. [PubMed: 10585229]
51. Hool K, Schuchardt B. A new instrument for the measurement of liquid-liquid interfacial tension and the dynamics of interfacial tension reduction. Measurement Science and Technology. 1992; 3:451.
52. Drummond C, Israelachvili J. Surface forces and wettability. Journal of Petroleum Science and Engineering. 2002; 33:123–133.
53. Lide, DR. CRC Handbook of Chemistry and Physics. 91. CRC Press; Cleveland, OH: 2011.
54. Eberhardt C, Grathwohl P. Time scales of organic contaminant dissolution from complex source zones: Coal tar pools vs. blobs. Journal of Contaminant Hydrology. 2002; 59:45–66. [PubMed: 12683639]
55. Chiwetelu CI, Hornof V, Neale GH. A dynamic-model for the interaction of caustic reagents with acidic oils. AICHE Journal. 1990; 36:233–241.
56. Nasr-El-Din HA, Hawkins BF, Green KA. Recovery of residual oil using the alkali/surfactant/polymer process: Effect of alkali concentration. Journal of Petroleum Science and Engineering. 1992; 6:381–401.
57. Touhami Y, Hornof V, Neale GH. Dynamic interfacial tension behavior of acidified oil/surfactant-enhanced alkaline systems 1. Experimental studies. Colloids and Surfaces A: Physiochemical and Engineering Aspects. 1998; 132:61–74.
58. Wasan, DT. Surfactant-enhanced alkaline flooding for light oil recovery: Annual report 1992–1993. 1994.
59. Chatterjee J, Wasan DT. A kinetic model for dynamic interfacial tension variation in an acidic oil/alkali/surfactant system. Chemical Engineering Science. 1998; 53:2711–2725.
60. Dwarakanath V, Jackson RE, Pope GA. Influence of wettability on the recovery of NAPLs from alluvium. Environmental Science and Technology. 2002; 36:227–231. [PubMed: 11827056]
61. Dong M, Ma S, Liu Q. Enhanced heavy oil recovery through interfacial instability: A study of chemical flooding for Brintnell heavy oil. Fuel. 2009; 88:1049–1056.
62. Wright DJ, Birak PS, Pedit JA, Miller CT. Effectiveness of source-zone remediation of DNAPL–contaminated subsurface systems. Journal of Environmental Engineering–ASCE. 2010; 136:452–465.

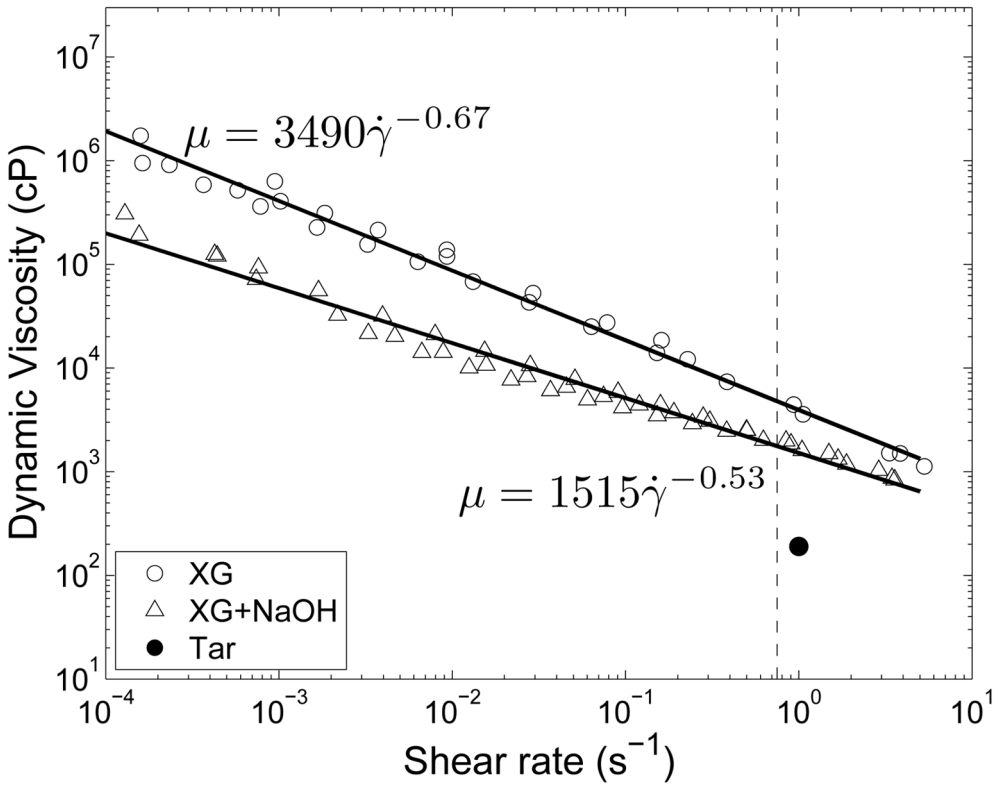

Figure 1.
Rheology of XG solutions. The results of three analyses and the best-fit power law equation for each solution are shown. The dashed line represents a shear rate of 0.75 s^{-1}

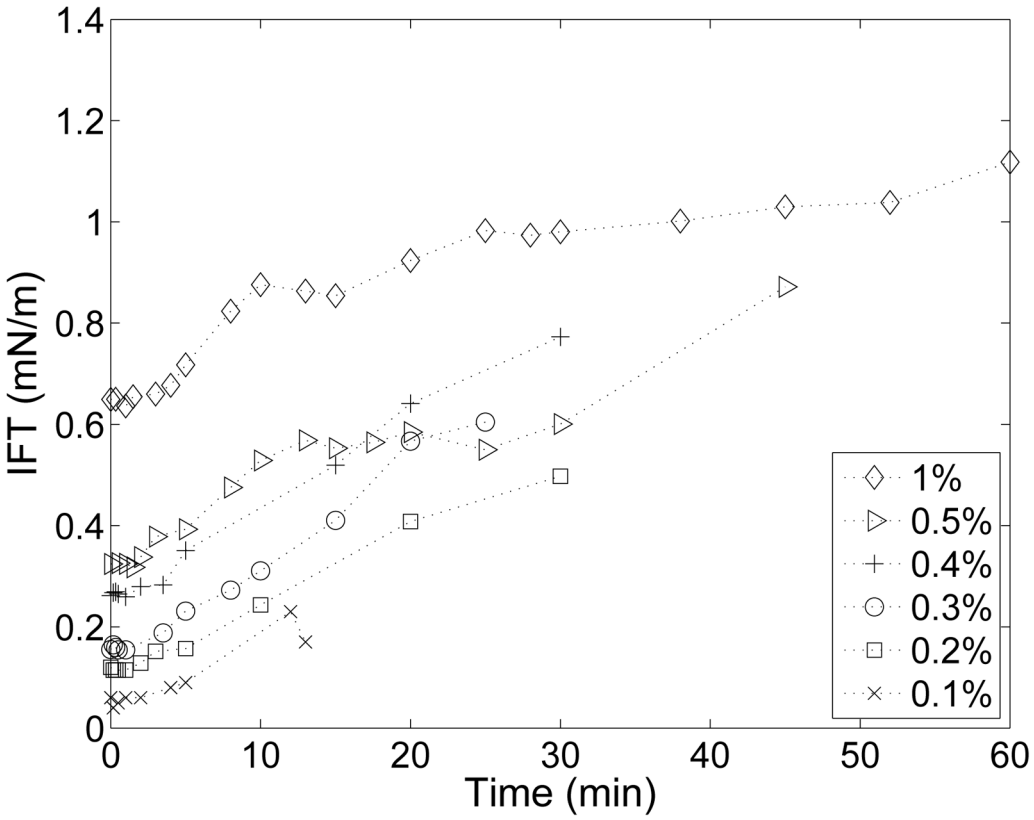

Figure 2.
Dynamic tar-water IFT. Each point is the average of duplicate values.

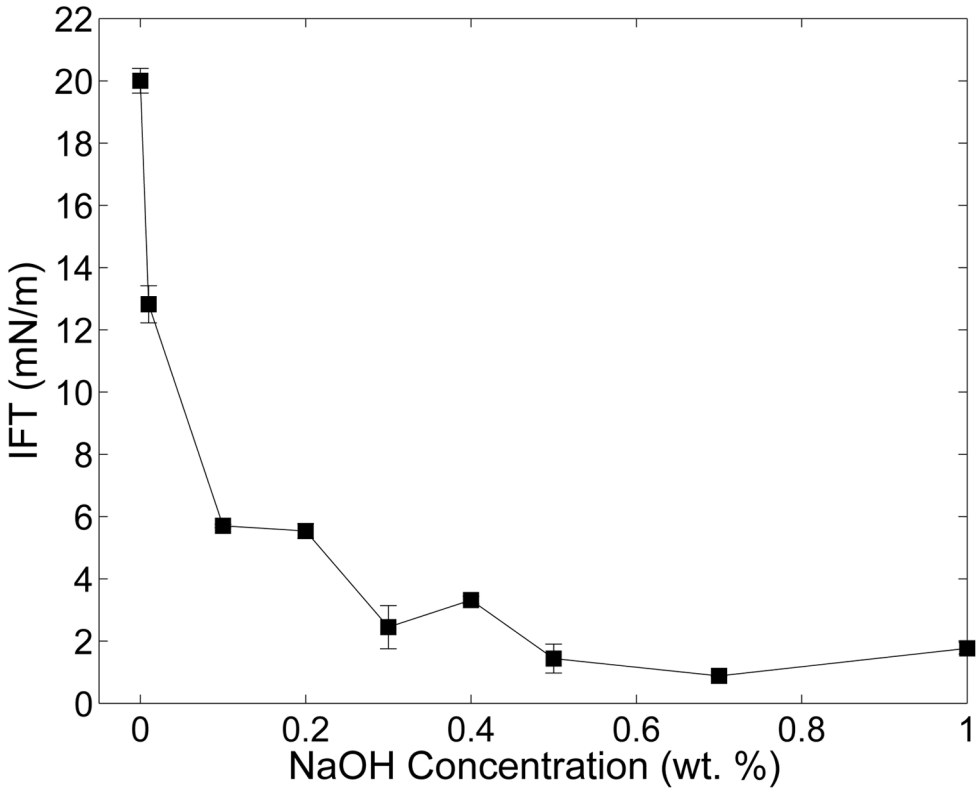

Figure 3.
Equilibrated tar-water IFTs for a range of NaOH concentrations. Error bars are the 95% CI.

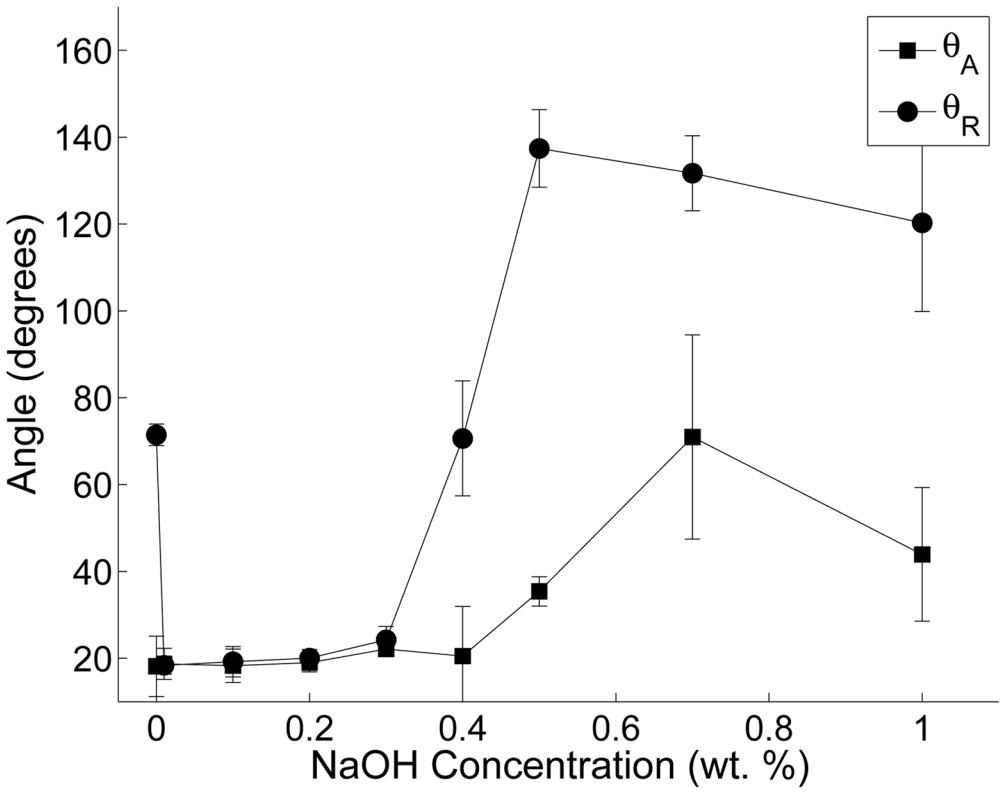

Figure 4.
Contact angle measurements. Error bars are the 95% CI.

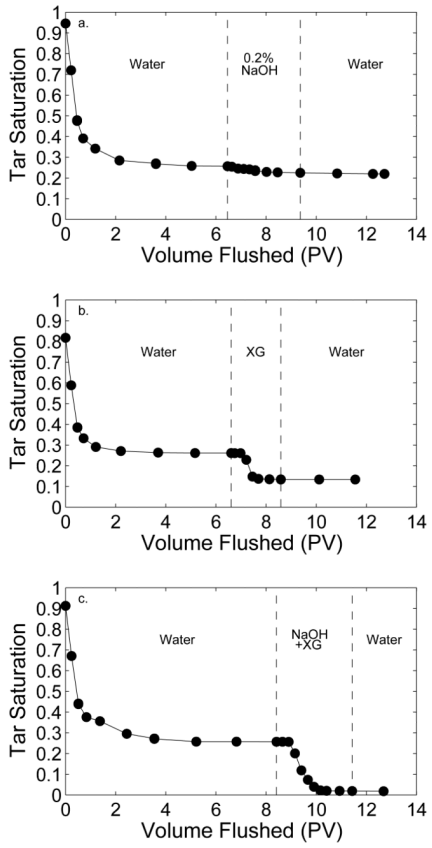

Figure 5.
Results of select column flushing experiments illustrating the improved tar removal for a combined NaOH + XG solution versus either NaOH or XG alone: (a) C1, 0.2% NaOH; (b) C4, 5000 ppm XG; (c) C5, 0.2% NaOH + 5000 ppm XG.

Table 1

Tar composition and properties. Compound concentrations are the average of 3 injections of 3 samples. All other values are the average of three analyses. All values are ± 95% CI

Compound	Concentration (mg/g)
indane	3.6 ± 0.1
indene	2.2 ± 0.1
naphthalene	95 ± 3
benzo(b)thiophene	3.9 ± 0.1
2-methylnaphthalene	34 ± 1
1-methylnaphthalene	24.4 ± 0.9
biphenyl	5.3 ± 0.2
2-ethylnaphthalene	4.5 ± 0.1
acenaphthylene	2.4 ± 0.1
acenaphthene	11.5 ± 0.4
dibenzofuran	4.1 ± 0.1
fluorene	10.9 ± 0.3
dibenzothiophene	5.5 ± 0.8
phenanthrene	33 ± 1
anthracene	8.9 ± 0.3
carbazole	3.0 ± 0.1
fluoranthene	13.0 ± 0.4
pyrene	14.7 ± 0.5
benzo(a)anthracene	5.3 ± 0.1
chrysene	6.0 ± 0.3
benzo(b)fluoranthene	3.5 ± 0.2
benzo(k)fluoranthene	3.5 ± 0.3
benzo(a)pyrene	4.5 ± 0.5
indeno(1,2,3-CD)pyrene	2.8 ± 0.2
dibenz(a,h)anthracene	1.2 ± 0.1
benzo(ghi)perylene	2.7 ± 0.3
sum	309 ± 4
asphaltenes	168 ± 3
extractable acids	1.8 ± 0.2
extractable bases	0.9 ± 0.3

Table 2

Summary of column experiment results.

Column	Flushing Solution	PV Flushed	Residual S_n	Final S_n	% Removal
C1	0.2% NaOH	2.7	0.26	0.22	15 %
C2	0.35% NaOH	7.0	0.26	0.15	44 %
C3	0.5% NaOH	2.9	0.26	0.24	10 %
C4	5000 ppm XG	3.5	0.26	0.13	51 %
C5	0.2% NaOH + 5000 ppm XG	3.0	0.26	0.018	93 %
C6	0.2% NaOH + 5000 ppm XG	3.2	0.32	0.037	87 %
C7	0.35% NaOH + 5000 ppm XG	2.5	0.28	0.037	85 %
C8	0.5% NaOH + 5000 ppm XG	1.9	0.25	0.048	81 %
C9	0.5% NaOH + 5000 ppm XG	2.3	0.29	0.043	85 %
C10	0.5% NaOH + 5000 ppm XG	2.7	0.29	0.046	84 %

Table 3

Aqueous phase concentrations before and after alkaline flushing. C_i^{eq} is the equilibrium concentration as calculated with Raoult's law. The pure compound aqueous solubilities (S_i^{aq}) are from (53) and the fugacity ratios (f^S/f^L) are from (54). All units are μg/L. ± 95% CI.

Compound	S_i^{aq}	f^S/f^L	C_i^{eq}	Preflush	Postflush
naphthalene	31600	0.3	21200	15300 ± 300	11200 ± 800
acenaphthene	3800	0.2	370	264 ± 3	270 ± 50
fluorene	1900	0.16	210	140.3 ± 0.2	140 ± 20
phenanthrene	1200	0.28	210	139 ± 7	130 ± 50
anthracene	44	0.01	57	24.8 ± 0.3	30 ± 2
fluoranthene	210	0.21	17	12 ± 3	18 ± 7
pyrene	13.9	0.11	2.5	10 ± 2	18 ± 5
benzo(a)anthracene	9.3	0.04	1.3	1.4 ± 0.2	4 ± 1
chrysene	1.9	0.0097	1.2	1.2 ± 0.1	3 ± 3
benzo(b)fluoranthene	1.5	0.039	0.16	< 0.16	< 0.16
benzo(k)fluoranthene	8.0	0.013	2.10	0.3 ± 0.6	1.6 ± 0.80
benzo(a)pyrene	4.3	0.03	0.61	1 ± 2	3 ± 2
dibenz(a,h)anthracene	0.5	0.004	0.09	< 0.16	< 0.16
benzo(g,h,i)perylene	0.26	0.003	0.14	0.3 ± 0.1	< 0.16
indeno(1,2,3-cd)pyrene	0.2	0.045	0.01	0.5 ± 0.5	< 0.16